frontiers in Nanotechnology

ORIGINAL RESEARCH
published: 14 October 2021
doi: 10.3389/fnano.2021.757487

Structured Copper Mesh for Efficient Oil-Water Separation Processed by Picosecond Laser Combined With Chemical Treatment or Thermal Oxidation

Zihang Liang[1,2], *Wanying He*[1,2], *Dongkai Chu*[1,2]*, *Shuoshuo Qu*[1,2] *and Peng Yao*[1,2]*

[1]*Center for Advanced Jet Engineering Technologies (CaJET), School of Mechanical Engineering, Shandong University, Jinan, China,* [2]*Key Laboratory of High Efficiency and Clean Mechanical Manufacture, Ministry of Education, Shandong University, Jinan, China*

Oil-water separation has great practical significance, and can be used to help cope with growing oily industrial sewage discharge or marine oil spills, avoiding water pollution. Smart artificial super-wettable materials used for oil-water separation have aroused enormous interest because of their advantages of energy efficiency and applicability across a wide range of industrial processes. Herein, we report a highly efficient, simple method for oil-water separation using copper mesh fabricated by picosecond laser processing combined with chemical treatment or thermal oxidation. After laser processing, the surfaces of copper mesh show superhydrophilicity (hydrophilicity) and underwater superoleophobicity, which can be used to separate water from oil. While, for the samples after laser and chemical treatment or laser treatment combined with thermal oxidation, the surfaces become superhydrophobic (hydrophobic) and underwater superoleophilic, which can separate oil from water. Moreover, these three kinds of super-wettability meshes show high separation efficiency, achieving more than 99% seperation. Furthermore, the as-prepared mesh can be used for various oil-water mixture separation, such as edible oil, kerosene, diesel, and so on. Thus, this work will provide insights for controllable oil-water separation, and will also be beneficial to the study of microfluidic devices, and smart filters.

Keywords: oil-water separation, copper mesh, picosecond laser, chemical treatment, thermal oxidation

OPEN ACCESS

Edited by:
Kai Yin,
Central South University, China

Reviewed by:
Faze Chen,
Tianjin University, China
Jiale Yong,
Xi'an Jiaotong University, China
Youwang Hu,
Central South University, China

***Correspondence:**
Dongkai Chu
chudongkai@sdu.edu.cn
Peng Yao
yaopeng@sdu.edu.cn

Specialty section:
This article was submitted to Nanophotonics, a section of the journal Frontiers in Nanotechnology

Received: *12 August 2021*
Accepted: *20 September 2021*
Published: *14 October 2021*

Citation:
Liang Z, He W, Chu D, Qu S and Yao P (2021) Structured Copper Mesh for Efficient Oil-Water Separation Processed by Picosecond Laser Combined With Chemical Treatment or Thermal Oxidation. Front. Nanotechnol. 3:757487. doi: 10.3389/fnano.2021.757487

1 INTRODUCTION

In the past few decades, as energy demand has grown, industrial oily sewage discharges and oil spill accidents have occurred frequently, well-known examples of such being the spills in The Gulf of Mexico and Alaska Harbor (Crone and Tolstoy, 2010; Yong et al., 2016a). Those accidents resulted in serious sea ecosystem pollution and huge economic losses. To deal with this problem, developing effective oil-water separation technologies and materials has been a hot topic in this area (Chu et al., 2015; Wang et al., 2014; Xue et al., 2014). Recently, superwetting materials with superoleophilic or superoleophobic (underwater superoleophobic) surfaces have gained increasing attention for use in selective oil adsorption and oil-water separation (Kong et al., 2015; Nishimoto and Bhushan, 2012;

Wang et al., 2016). Among them, mesh materials have been widely applied in separating oil-water mixtures (Song et al., 2014; Song et al., 2015). For example, Feng et al. found that after being coated with polytetrafluoroethylene, the metal mesh showed both superhydrophobicity (hydrophobicity) and superoleophilicity in air that can be used to separate a mixture of oil and water (Feng et al., 2004). Xue, et al. studied a polyacrylamide hydrogel-coated mesh for oil-water separation. Due to the surfaces of the mesh showing superhydrophilicity and underwater superoleophobicity, it could prevent the oil from touching the surface, achieving a high reusability rate (Xue et al., 2011). Liu, et al. reported an underwater superoleophobic wire mesh prepared by coating a thin layer of the graphene oxide film that can be used in the separation of bean oil from water (Liu et al., 2015). Cheng, et al. demonstrated that by simply assembling responsive thiol molecules on structured copper mesh, a smart pH-controllable oil/water separating membrane can be prepared. The as-prepared mesh shows superhydrophobicity (hydrophobicity) in non-alkaline water, whereas it becomes superhydrophilic for alkaline water (Cheng et al., 2015).

Although these explorations have extensively advanced the development of oil-water separation, these chemical reagents are harmful to the environment and the coatings are prone to degradation. As a result, the samples are difficult to be use many times. In the past decade, laser direct processing technology has attracted considerable attention due to its unique advantages in processing superwetting surfaces, such as substrate-independent, and high accuracy (Chu et al., 2018; Yin et al., 2018; Chu et al., 2019a; Chu et al., 2019b; Yang et al., 2019; Wu et al., 2021). As such, Yong, et al. processed a durable superhydrophobicity and superoleophilicity PTFE surface by using a femtosecond laser. Through subsequent mechanical drilling processes, the as-prepared PTFE film could be applied in oil-water separation (Yong et al., 2016b). Li, et al. presented a multifunctional ultrathin aluminum foil realized by one-step femtosecond laser irradiation, which showed underwater superoleophobic ability and oil-water separation function (Li et al., 2016). Yin, et al. introduced a simple method to fabricate superwetting stainless steel mesh surfaces with one-step femtosecond laser processing. The meshes show high separation efficiency even after the abrasion tests and corrosion tests (Yin et al., 2017). Nevertheless, the femtosecond laser ablation still shows low processing efficiency and the machine is highly expensive, being about four times more expensive than picosecond lasers, leading them difficult to use widely in industry. Thus, a cheaper and highly efficient processing method for superwetting surfaces is highly desired.

Herein, by using picosecond laser processing combined with chemical treatment (CT) or thermal oxidation (TO), we obtain two types of superwetting surfaces: one shows superhydrophilicity (underwater superoleophobicity), which can be used to separate water from oil, while the other one shows superhydrophobicity (hydrophobicity) and underwater superoleophilicity, which can be used to separate oil from water. The as-prepared meshes show high separation efficiency (more than 99%) for different oil-water mixtures. This cheaper and highly efficient method for oil-water separation surfaces processing may hold great promise for the treatment of sewage.

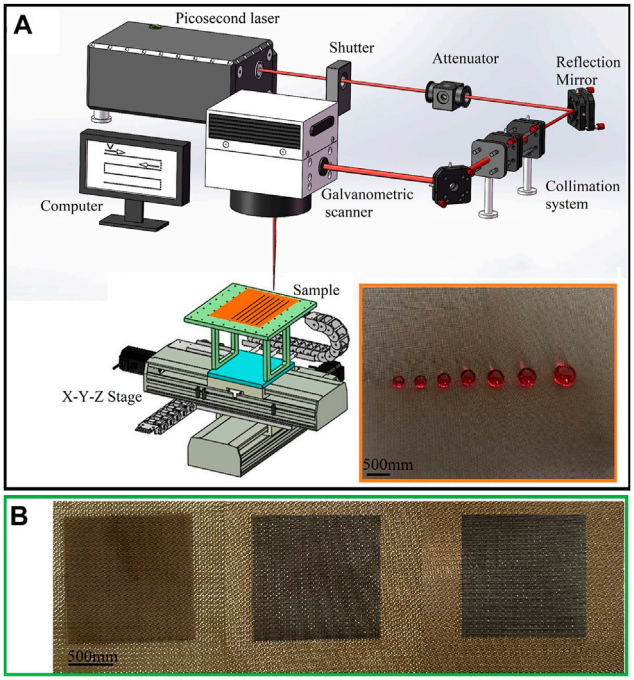

FIGURE 1 | The schematic of experiment setup **(A)** and the sample after LT, LCT, and LTCTO**(B)**.

2 EXPERIMENTAL SETUP

2.1 Laser Processing

Figure 1A shows the schematic of the experiment setup. A copper mesh with a dimension of 6 × 5 cm^2 is initially mounted on a computer-controlled 3-dimensional platform. A picosecond laser with a wavelength of 1,064 nm, repetition of 100 kHz, pulse duration of 15 ps is used. The single pulse energy is held constant at 310 μJ/cm^2. The laser beam is focused by a two-mirror galvanometric scanner (AXIALSCAN-20-DIGITA-II-Y200, RAYLASE, Germany) with an F-Theta lens (f = 326 mm) on the sample surface after passing through the collimation system (keeping the light parallel), shutter (a switch to pass or block the laser pulse), and attenuator (consists of a half-wave plate and a linear polarizer to control the laser energy). The copper mesh samples are line-by-line scanned at air and room temperature. The scanning speed and the interval of adjacent laser scanning lines are adjusted by the mechanical platform. After laser processing, the samples are cleaned with alcohol and deionized water in an ultrasonic bath at room temperature for 10 min each.

2.2 Chemical Treatment or Thermal Oxidation

The typical low-surface-energy treatment of fluoroalkylsilane modification is adopted here (Chu et al., 2021). The laser-ablated samples are immersed in a 1% fluoroalkylsilane (1H,1H,2H,2H- perfluorodecyltriethoxysilane) solution (in

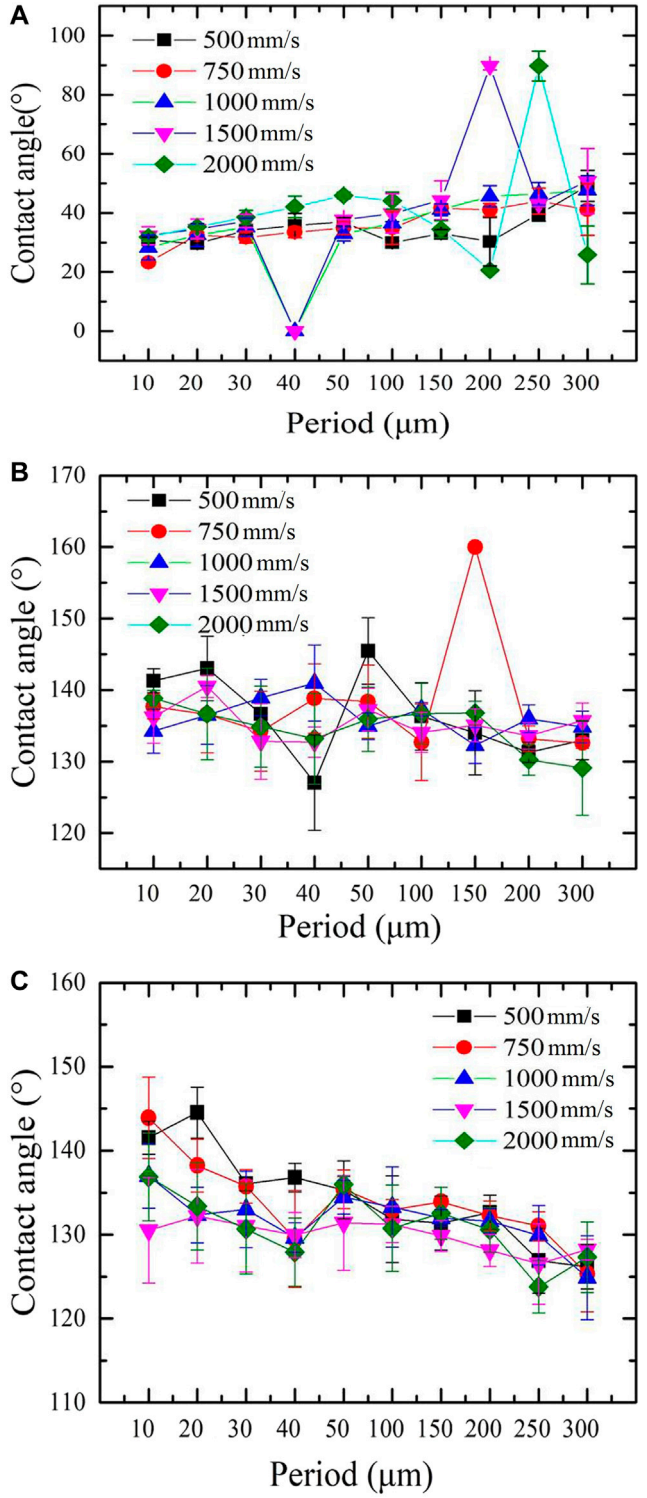

FIGURE 2 | CA for different treated samples. **(A)** After laser treatment. **(B)**After laser and chemical treatment. **(C)**After laser treatment combined with thermal oxidation.

ethanol) for 1 day. After the sample is immersed in the fluoroalkylsilane solution, hydrolysis and condensation reactions will occur, and the sample surface will self-assemble to form a single or multi-molecular film. Then, the samples are rinsed with ethanol to remove the excess fluoroalkylsilane molecules and heated at 60°C for 15 min.

After being laser processed some of the copper meshes are heated at 300°C for 2 h in a muffle furnace.

2.3 Characterization

The morphology of the copper mesh sample was characterized using a scanning electron microscope (SEM, JSM-7610F, JEOL). The element composition of the sample was analyzed through energy-dispersive X-ray spectroscopy ((EDS, JSM-7610F, JEOL). The contact angle and sliding angle of water (CA, SA) and oil (OCA, OSA) droplets were measured by a contact-angle system (SDC-200S, SINDIN).

2.4 Oil-Water Separation

During the oil-water separation, the processed copper mesh is tilted about 10°. The as-prepared mesh is prewetted with water or oil. The mixtures of diesel (edible oil, kerosene, hexadecane, 1,2-dichloroethane) and water are poured onto the as-prepared mesh. In order to provide a clearer observation, the water used wa dyed by Sudan III, which exhibits a red color.

3 RESULTS AND DISCUSSION

Figure 1B shows a digital photo of copper mesh surfaces after laser treatment (LT), laser and chemical treatment (LCT), and laser treatment combined with thermal oxidation (LTCTO). It can be clearly seen that the pristine untreated copper meshes show brilliant yellow, while the treated areas exhibit black, which is because the micro/nano-structures are formed on the mesh surface. The as-prepared surface after LCT or LTCTO can repel water droplets with a volume ranging from 6 to 15 μl, as shown in the inset picture of **Figure 1A**. For the pristine copper mesh, the CA is 127° ± 2.3°. By using this processing system, a 1.5 × 1.5 cm^2 region is processed in less than 1 min (the scanning speed and scanning period is 1,000 mm/s and 10 μm, respectively), which is quicker than previous studies (Duan et al., 2018; Kai et al., 2018; Yong et al., 2018; Yong et al., 2021).

Figure 2 shows the relationships between the scanning period (scanning speed) and the mesh surfaces' (after LT, LCT, and LTCTO) CA of water with a volume of 6 μl. It can be seen that after LT, the surfaces show superhydrophilicity (hydrophilicity, **Figure 2A**). When the scanning period increases, the CA increases, though ultimately the scanning speed has little effect on the CA. When the scanning speed and scanning period is 1,000 mm/s (1,500 mm/s) and 40 μm, respectively, the as-prepared surfaces show superhydrophilicity. When a water droplet is in contact with the surfaces, the water can easily enter into the structured surfaces and then quickly spread out (**Supplementary Movie S1**). After LCT, the copper mesh surfaces show superhydrophobicity (hydrophobicity, **Supplementary Movie S2**). As the scanning speed and period increase, the CA stays around 135°, except for when the scanning speed and period are 750 mm/s and 150 μm, respectively. For the sample after

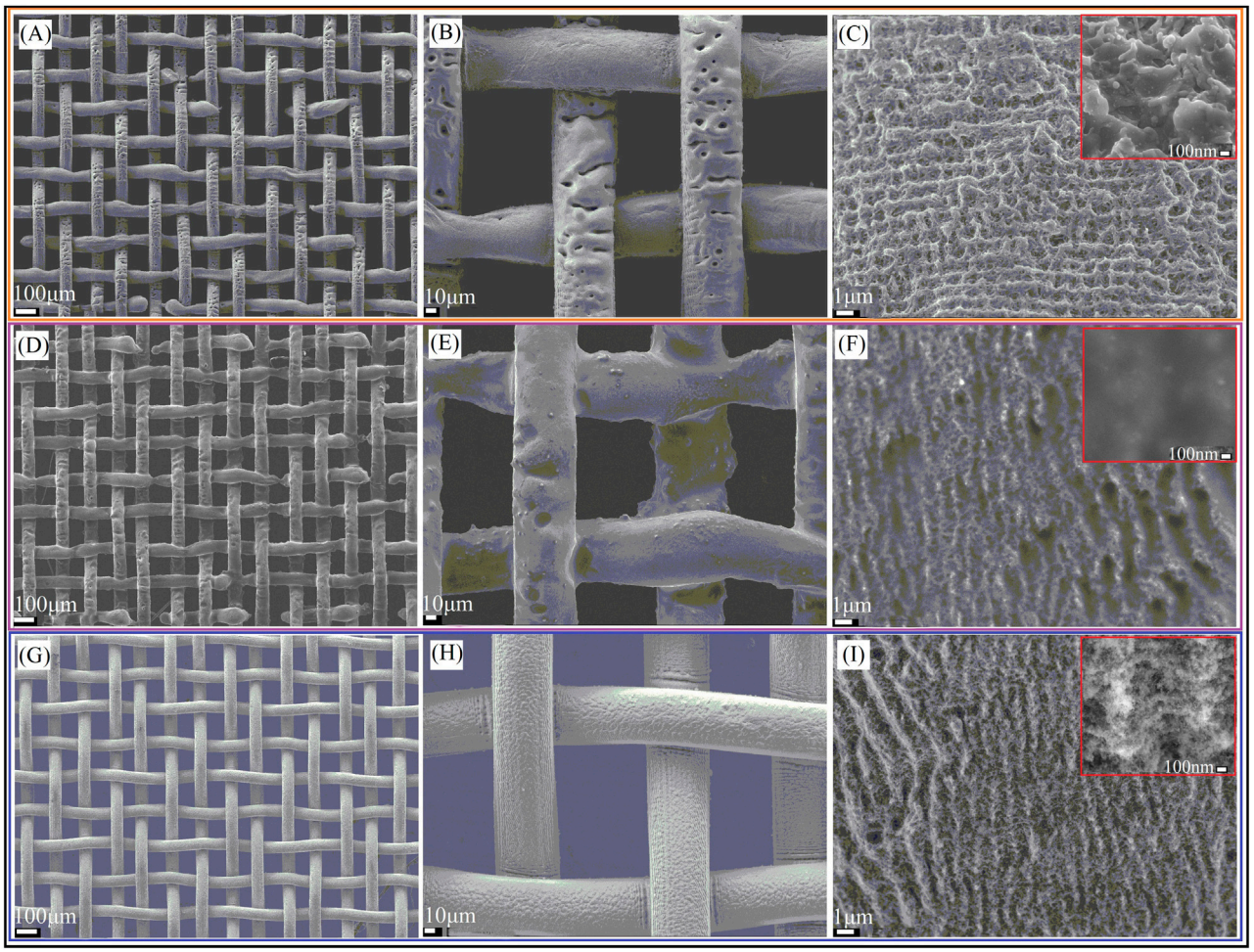

FIGURE 3 | SEM images for different treated sample. **(A–C)** After LT. **(D–F)**After LCT. **(G–I)**After LTCTO.

LTCTO, the surfaces show hydrophobicity. When the scanning period increases, the CA decreases. When the period is smaller than 50 μm, the CA increases along with the scanning speed.

Figure 3 shows the SEM images of samples after three different treatment methods (LT, LCT, and LTCTO). The SEM images for pristine copper mesh and the mesh after CT and TO are shown in **Supplementary Figure S1**. It shows that the pristine copper is relatively smooth. After CT, the surface is plated with a layer of uneven film, leading to poor conductivity. After TO, the surface remains fundamentally unchanged. **Figures 3A–C** shows the SEM image after LT at different magnifications. It can be clearly seen that the as-prepared surface is characterized by some uneven micro-hole structures and hierarchical, periodic ripple structures. After LCT, the sample surface will self-assemble to form a single or multi-molecular film. The outside of this film is covered by (-CF3), and experiments have proved that (-CF3) has good hydrophobic properties. As a result, the nanostructures that occurred in **Figure 3C** will be blocked as shown in **Figures 3D–F**, only some micro-sized structures can be retained. Many burrs occurred on the surface of the mesh prepared by LTCTO, the average size of each burr being about 10 nm, which can be seen from **Figures 3G–I** (**Supplementary Figure S2**). Compared with the surfaces treated by LT, the surfaces prepared by LTCTO filled with numerous snow-like structures. In addition, samples processed with different periods have different burr growth situations. The smaller the period, the longer the burr grows. The chemical compositions of the pristine and as-prepared copper mesh are studied in **Figure 4**. The main elements of pristine copper are Cu, Zn, and a bit of C and O. After LT, the content of O and C increase significantly. While for samples after CT and LCT, the element of O is replaced by F. Furthermore, the content of F in the sample prepared by LCT (8.6%) is more than that of the sample prepared by CT (1.1%). Compared with pristine copper mesh, the oxygen content for the sample after TO and LTCTO both increased, with an increment of 3.1 and 15.9%. respectively.

Figure 5A shows the underwater superoleophobicity of the as-prepared sample (after LT). It can be clearly seen that the oil droplet on the copper mesh after LT can keep an approximately spherical shape with the OCA of 161° ± 1.4°. In addition, the surface adhesion of the as-prepared sample for oil droplets is ultralow (**Supplementary Movie S3**). The oil droplet can also roll away from the as-prepared mesh with a low sliding angle. **Figure 5B** shows the CA/SA as a function of various fluids as sampled after LT, LCT, LTCTO. For the sample after

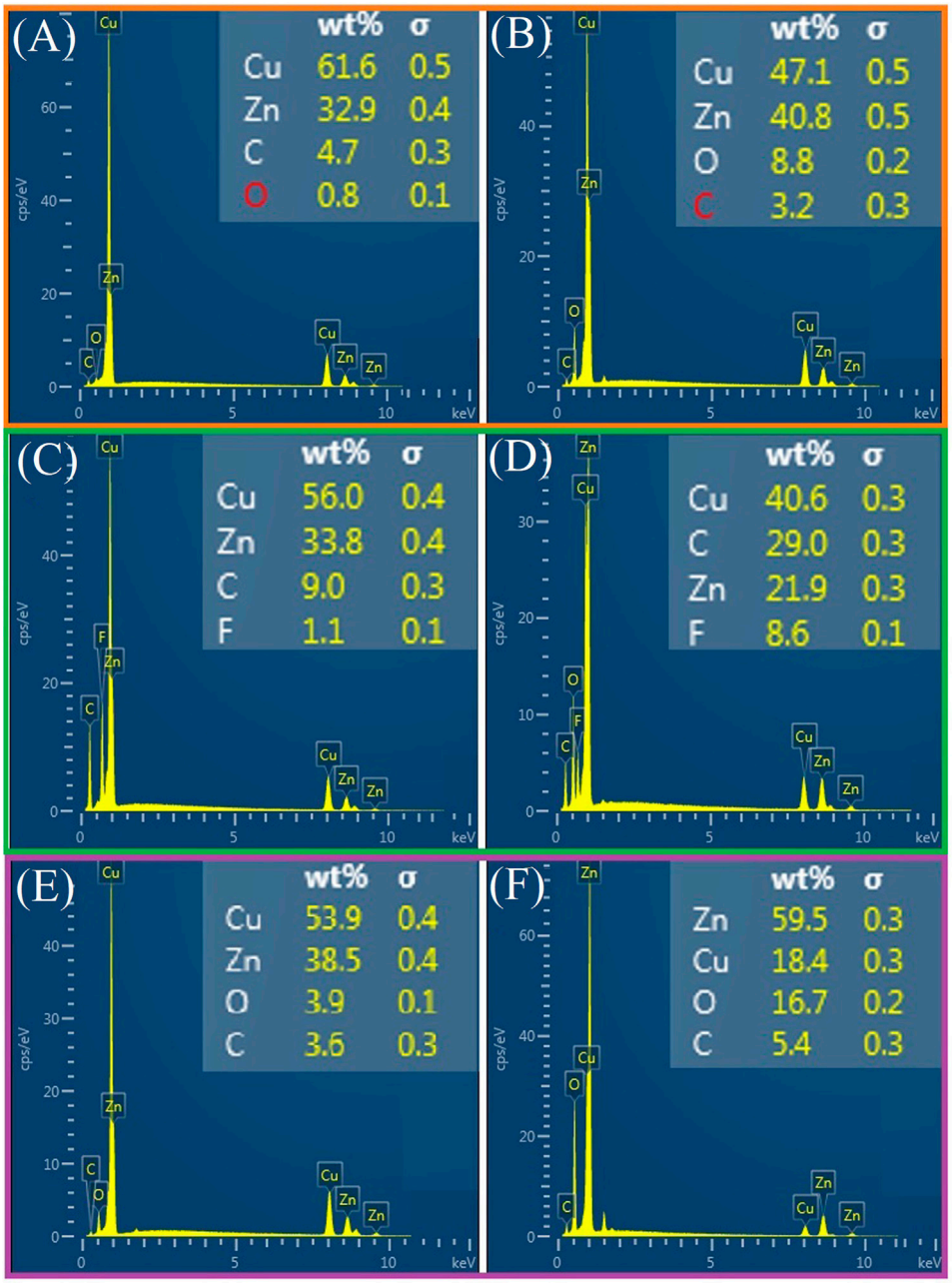

FIGURE 4 | EDS spectra for different treated samples. **(A)** The main elements of pristine copper. **(B)** The main elements of copper mesh after LT. **(C)** The main elements of copper mesh after CT. **(D)** The main elements of copper mesh after LCT. **(E)** The main elements of copper mesh after TO. **(F)** The main elements of copper mesh after LTCTO.

LT, the surfaces show superhydrophilicity and underwater superoleophobicity, the OCA values for these oils (edible oil, kerosene, hexadecane, 1,2-dichloroethane) range from 158° to 162.5°, and the OSAs are all less than 20°. For the samples after LCT and LTCTO, it becomes superhydrophobic (hydrophobic) and underwater superoleophilic. The oil droplets cannot roll off from the surface even if it is placed upright. **Figures 5C–E** exhibits the oil-water separating process using the mesh fabricated by LT. A copper mesh sample with a dimension of 6 × 5 cm^2 is processed with scanning speed and scanning period of 1,500 mm/s and 40 μm, respectively. After being cleaned with deionized water, it is wetted by water. Then the wetted sample was put on two beakers with a tilted angle of 10° and a mixture of kerosene oil and water poured over, which mimics an oil spill, onto the upper side of the sample. Due to the force of gravity, kerosene can quickly flow over the as-prepared mesh and pour into the left beaker. This can be attributed to the underwater superoleophobic and low oil-adhesion properties of the laser-treated surface. Meanwhile, water can permeate through the as-

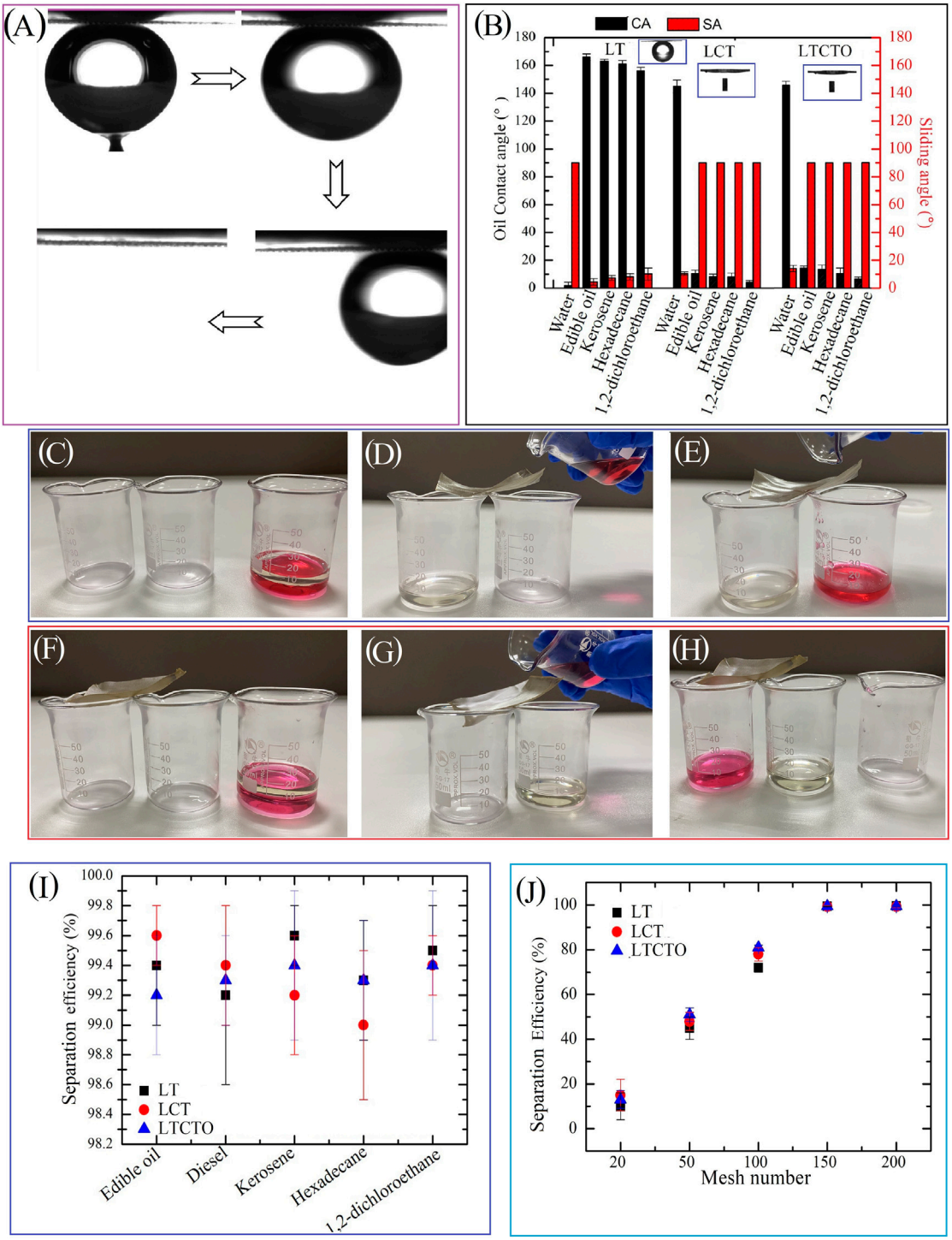

FIGURE 5 | Wettability and separation efficiency of three different prepared mesh for various oils and mesh numbers, respectively. **(A)** Underwater oil droplet rolling on the laser-treated copper mesh surface. **(B)** CA/SA as a function of various fluid of sample after LT, LCT, and LTCTO. **(C–H)** Digital images for oil-water separation processing using the copper mesh after LT and LTCTO **(I)** Separation efficiency as a function of various oil samples after LT, LCT, and LTCTO. **(J)** Separation efficiency as a function of different mesh numbers of samples after LT, LCT, and LTCTO.

prepared superhydrophilic mesh and drop into the right beaker (**Supplementary Movie S4**, this can be called the separation of oil from water), as shown in **Figures 5C–E**. Additionally, due to the fact that any oil remaining on the as-prepared mesh is easily washed away by water (underwater superolephobicity), the oil-water separation system can be reused many times. For the sample after LCT and

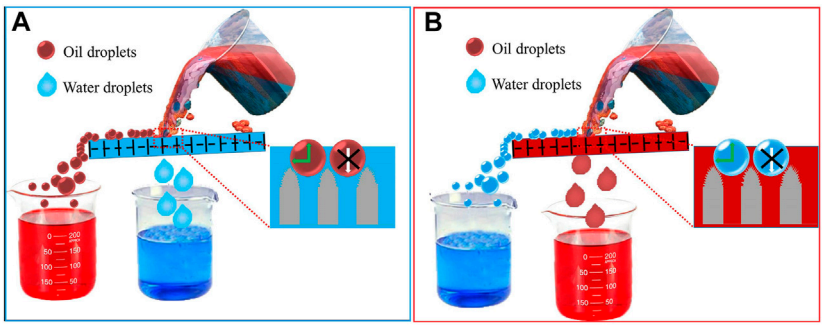

FIGURE 6 | Schematic of the possible mechanism of the as-prepared (LT, LCT, or LTCTO) copper mesh for oil-water separation.

LTCTO, because of its superhydrophobicity (hydrophobic), it should be wetted by oil. Then repeat the above steps, interestingly, we find that the kerosene will permeate through the as-prepared surfaces and drop into the right beaker, while water will go to the left beaker (called separating water from oil, **Supplementary Movie S5**), as shown in **Figures 5F–H**. The separation efficiency of the sample after LT for the edible oil/water, diesel/water, kerosene/water, hexadecane/water, and 1,2-dichloroethane/water mixture is 99.4%, 99.2%, 99.6%, 99.3%, and 99.5%, respectively. For samples after LCT and LTCTO, the separation efficiency is also more than 99%, as shown in **Figure 5I**. It indicates that the as-prepared three different mesh samples all can be used for the highly efficient oil-water separation. The relationship between the separation efficiency and mesh number is revealed in **Figure 5J**. It can be clearly seen that only if the mesh number is larger than 150 can a higher (>99%) separation efficiency can be obtained.

Figure 6 presents a possible mechanism for the oil-water separation using the as-prepared copper mesh. For the sample prepared by LT, a water film will form on the processed sample surface after pre-wetting, which can be attributed to the superhydrophilicity (hydrophilicity) of the as-prepared surfaces. Combined with underwater superoleophobicity, the as-prepared surfaces can prevent the oil droplets from contacting the copper mesh, while allowing water to pass through the mesh under the downward capillary force driven by superhydrophilicity (hydrophilicity) and the force of gravity (Yang et al., 2019). It is difficult for oil droplets to pass through the sample, and they can only roll away along the surfaces. Finally, oil-water separation is achieved. For the samples prepared by LCT or LTCTO, an oil film will form on the prepared surfaces, which will prevent water contact the copper mesh, resulting in the oil being able to pass through the mesh, while the oil cannot, thus, achieving the purpose of separating an oil-water mixture.

4 CONCLUSION

In summary, we report three different kinds of oil-water separation copper mesh processed by picosecond laser combined with chemical treatment or thermal oxidation. It is found that after laser processing, the copper mesh surfaces show superhydrophilicity and underwater superoleophobicity, which can be used to separate water from oil. While after chemical treatment or thermal oxidation, the surfaces become superhydrophobic (hydrophobic) and underwater superoleophilic, which can separate oil from water. The separation efficiency for these three as-prepared samples can reach more than 99% for various oil-water mixtures. These cheaper and highly efficient methods for oil-water separation surface processing may hold great promise for the treatment of sewage.

DATA AVAILABILITY STATEMENT

The original contributions presented in the study are included in the article/**Supplementary Material**, further inquiries can be directed to the corresponding authors.

AUTHOR CONTRIBUTIONS

ZL: Conceptualization, Investigation: WH and DC Formal analysis, Writing—original draft. SQ and PY Visualization, Writing—review and editing, Supervision. All authors contributed to the article and approved the submitted version.

FUNDING

Parts of this work are funded by the National Natural Science Foundation of China (no. 52075302), Shandong Provincial Natural Science Foundation (no. ZR2018MEE019), and Major Basic Research of Shandong Provincial Natural Science Foundation (no. ZR2018ZB0521, ZR2018ZA0401). The Fundamental Research Funds of Shandong University (2020GN049).

SUPPLEMENTARY MATERIAL

The Supplementary Material for this article can be found online at: https://www.frontiersin.org/articles/10.3389/fnano.2021.757487/full#supplementary-material

REFERENCES

Cheng, Z., Wang, J., Lai, H., Du, Y., Hou, R., Li, C., et al. (2015). PH-Controllable On-Demand Oil/Water Separation on the Switchable Superhydrophobic/Superhydrophilic and Underwater Low-Adhesive Superoleophobic Copper Mesh Film. *Langmuir* 31 (4), 1393–1399. doi:10.1021/la503676a

Chu, D., Singh, S. C., Yong, J., Zhan, Z., Sun, X., Duan, J. A., et al. (2019a). Superamphiphobic Surfaces with Controllable Adhesion Fabricated by Femtosecond Laser Bessel Beam on PTFE. *Adv. Mater. Inter.* 6 (14), 1900550. doi:10.1002/admi.201900550

Chu, D., Sun, X., Hu, Y., and Duan, J.-A. (2019b). Substrate-Independent, Switchable Bubble Wettability Surfaces Induced by Ultrasonic Treatment. *Soft Matter* 15 (37), 7398–7403. doi:10.1039/c9sm01404g

Chu, D., Yao, P., and Huang, C. (2021). Anti-Reflection Silicon with Self-Cleaning Processed by Femtosecond Laser. *Opt. Laser Technol.* 136, 106790. doi:10.1016/j.optlastec.2020.106790

Chu, Z., Feng, Y., and Seeger, S. (2015). Oil/Water Separation with Selective Superantiwetting/Superwetting Surface Materials. *Angew. Chem. Int. Ed.* 54 (8), 2328–2338. doi:10.1002/anie.201405785

Crone, T. J., and Tolstoy, M. (2010). Magnitude of the 2010 Gulf of Mexico Oil Leak. *Science* 330 (6004), 634. doi:10.1126/science.1195840

Chu, D., Yin, K., Dong, X. R., Luo, Z., Song, Y. X., and Duan, J. A. (2018). Ablation Enhancement by Defocused Irradiation Assisted Femtosecond Laser Fabrication of Stainless alloy. *Chin. Opt. Lett.* 16 (1), 011401. doi:10.3788/COL201816.011401

Duan, J.-A., Dong, X., Yin, K., Yang, S., and Chu, D. (2018). A Hierarchical Superaerophilic Cone: Robust Spontaneous and Directional Transport of Gas Bubbles. *Appl. Phys. Lett.* 113 (20), 203704. doi:10.1063/1.5054623

Feng, L., Zhang, Z., Mai, Z., Ma, Y., Liu, B., Jiang, L., et al. (2004). A Super-Hydrophobic and Super-Oleophilic Coating Mesh Film for the Separation of Oil and Water. *Angew. Chem. Int. Ed.* 43, 2012–2014. doi:10.1002/anie.200353381

Kong, L.-H., Chen, X.-H., Yu, L.-G., Wu, Z.-S., and Zhang, P.-Y. (2015). Superhydrophobic Cuprous Oxide Nanostructures on Phosphor-Copper Meshes and Their Oil-Water Separation and Oil Spill Cleanup. *ACS Appl. Mater. Inter.* 7 (4), 2616–2625. doi:10.1021/am507620s

Li, G., Fan, H., Ren, F., Zhou, C., Zhang, Z., Xu, B., et al. (2016). Multifunctional Ultrathin Aluminum Foil: Oil/Water Separation and Particle Filtration. *J. Mater. Chem. A.* 4, 18832–18840. doi:10.1039/C6TA08231A

Liu, Y.-Q., Zhang, Y.-L., Fu, X.-Y., and Sun, H.-B. (2015). Bioinspired Underwater Superoleophobic Membrane Based on a Graphene Oxide Coated Wire Mesh for Efficient Oil/Water Separation. *ACS Appl. Mater. Inter.* 7 (37), 20930–20936. doi:10.1021/acsami.5b06326

Nishimoto, S., and Bhushan, B. (2012). Bioinspired Self-Cleaning Surfaces with Superhydrophobicity, Superoleophobicity, and Superhydrophilicity. *RSC Adv.* 3 (3), 671–690. doi:10.1039/c2ra21260a

Song, J., Huang, S., Lu, Y., Bu, X., Mates, J. E., Ghosh, A., et al. (2014). Self-Driven One-Step Oil Removal from Oil Spill on Water via Selective-Wettability Steel Mesh. *ACS Appl. Mater. Inter.* 6 (22), 19858–19865. doi:10.1021/am505254j

Song, J., Lu, Y., Luo, J., Huang, S., Wang, L., Xu, W., et al. (2015). Oil Spills: Barrel-Shaped Oil Skimmer Designed for Collection of Oil from Spills (Adv. Mater. Interfaces 15/2015). *Adv. Mater. Inter.* 2, a–n. doi:10.1002/admi.201570077

Wang, B., Liang, W., Guo, Z., and Liu, W. (2014). Biomimetic Super-lyophobic and Super-lyophilic Materials Applied for Oil/water Separation: A New Strategy beyond Nature. *Chem. Soc. Rev.* 44 (1), 336–361. doi:10.1039/C4CS00220B

Wang, Y., Lin, F., Dong, Y., Liu, Z., Li, W., and Huang, Y. (2016). A Multifunctional Polymeric Nanofilm with Robust Chemical Performances for Special Wettability. *Nanoscale* 8 (9), 5153–5161. doi:10.1039/C5NR07601C

Wu, Z., Yin, K., Wu, J., Zhu, Z., Duan, J.-A., and He, J. (2021). Recent Advances in Femtosecond Laser-Structured Janus Membranes with Asymmetric Surface Wettability. *Nanoscale* 13, 2209–2226. doi:10.1039/D0NR06639G

Xue, Z., Cao, Y., Liu, N., Feng, L., and Jiang, L. (2014). Special Wettable Materials for Oil/water Separation. *J. Mater. Chem. A.* 2 (8), 2445–2460. doi:10.1039/c3ta13397d

Xue, Z., Wang, S., Lin, L., Chen, L., Liu, M., Feng, L., et al. (2011). A Novel Superhydrophilic and Underwater Superoleophobic Hydrogel-Coated Mesh for Oil/Water Separation. *Adv. Mater.* 23 (37), 4270–4273. doi:10.1002/adma.201102616

Yang, S., Yin, K., Wu, J., Wu, Z., Chu, D., He, J., et al. (2019). Ultrafast Nano-Structuring of Superwetting Ti Foam with Robust Antifouling and Stability towards Efficient Oil-In-Water Emulsion Separation. *Nanoscale* 11, 17607–17614. doi:10.1039/C9NR04381K

Yin, K., Chu, D., Dong, X., Wang, C., Duan, J.-A., and He, J. (2017). Femtosecond Laser Induced Robust Periodic Nanoripple Structured Mesh for Highly Efficient Oil-Water Separation. *Nanoscale* 9, 14229–14235. doi:10.1039/C7NR04582D

Yin, K., Luo, Z., Du, H., Dong, X., and Duan, J.-A. (2018). Femtosecond Laser Fabrication of a Gradient-Wettability Mesh for Spilled Oil Crossflow Collection. *Mater. Lett.* 215, 272–275. doi:10.1016/j.matlet.2017.12.130

Yin, K., Yang, S., Dong, X., Chu, D., Duan, J.-A., and He, J. (2018). Ultrafast Achievement of a Superhydrophilic/Hydrophobic Janus Foam by Femtosecond Laser Ablation for Directional Water Transport and Efficient Fog Harvesting. *ACS Appl. Mater. Inter.* 10, 31433–31440. doi:10.1021/acsami.8b11894

Yong, J., Chen, F., Li, W., Huo, J., Fang, Y., Yang, Q., et al. (2018). Underwater Superaerophobic and Superaerophilic Nanoneedles-Structured Meshes for Water/Bubbles Separation: Removing or Collecting Gas Bubbles in Water. *Glob. Challenges* 2 (4), 1700133. doi:10.1002/gch2.201700133

Yong, J., Chen, F., Yang, Q., Bian, H., Du, G., Shan, C., et al. (2016a). Oil-Water Separation: A Gift from the Desert. *Adv. Mater. Inter.* 3 (7), 1500650. doi:10.1002/admi.201500650

Yong, J., Fang, Y., Chen, F., Huo, J., Yang, Q., Bian, H., et al. (2016b). Femtosecond Laser Ablated Durable Superhydrophobic PTFE Films with Micro-Through-Holes for Oil/water Separation: Separating Oil from Water and Corrosive Solutions. *Appl. Surf. Sci.* 389, 1148–1155. doi:10.1016/j.apsusc.2016.07.075

Yong, J., Yang, Q., Huo, J., Hou, X., and Chen, F. (2021). Superwettability-Based Separation: From Oil/Water Separation to Polymer/Water Separation and Bubble/Water Separation. *Nano Select* 2, 1580–1588. doi:10.1002/nano.202000246

Conflict of Interest: The authors declare that the research was conducted in the absence of any commercial or financial relationships that could be construed as a potential conflict of interest.

Publisher's Note: All claims expressed in this article are solely those of the authors and do not necessarily represent those of their affiliated organizations, or those of the publisher, the editors and the reviewers. Any product that may be evaluated in this article, or claim that may be made by its manufacturer, is not guaranteed or endorsed by the publisher.